NUCL SCI TECH (2018) 29:178
https://doi.org/10.1007/s41365-018-0515-9

Astrophysical constraints on a parametric equation of state for neutron-rich nucleonic matter

Nai-Bo Zhang[1,2] · Bao-An Li[2]

Received: 5 September 2018 / Revised: 25 October 2018 / Accepted: 25 October 2018 / Published online: 17 November 2018

Abstract Extracting the equation of state (EOS) and symmetry energy of dense neutron-rich matter from astrophysical observations is a long-standing goal of nuclear astrophysics. To facilitate the realization of this goal, the feasibility of using an explicitly isospin-dependent parametric EOS for neutron star matter was investigated recently in [1–3]. In this contribution, in addition to outlining the model framework and summarizing the most important findings from [1–3], we report a few new results regarding constraining parameters characterizing the high-density behavior of nuclear symmetry energy. In particular, the constraints on the pressure of neutron star matter extracted from combining the X-ray observations of the neutron star radius, the minimum–maximum mass $M = 2.01\ \mathrm{M}_{\odot}$, and causality condition agree very well with those extracted from analyzing the tidal deformability data by the LIGO + Virgo Collaborations. The limitations of using the radius and/or tidal deformability of neutron stars to constrain the high-density nuclear symmetry energy are discussed.

Keywords Neutron star · Equation of state · Symmetry energy

NBZ was supported in part by the China Scholarship Council. BAL acknowledges the U.S. Department of Energy, Office of Science, under Award Number DE-SC0013702, the CUSTIPEN (China-U.S. Theory Institute for Physics with Exotic Nuclei) under the U.S. Department of Energy Grant No. DE-SC0009971 and the National Natural Science Foundation of China under Grant No. 11320101004.

✉ Bao-An Li
Bao-An.Li@Tamuc.edu

1 Shandong Provincial Key Laboratory of Optical Astronomy and Solar-Terrestrial Environment, School of Space Science and Physics, Institute of Space Sciences, Shandong University, Weihai 264209, China

2 Department of Physics and Astronomy, Texas A&M University-Commerce, Commerce, TX 75429, USA

1 Introduction

In this mini-review as our contribution to the conference proceedings, we present some new results along with the most important findings originally reported in [1–3]. For more detailed discussions of our recent work on this topic, we refer the readers to [1–3].

As one of the most exotic objects in the universe, several extreme conditions, such as high density [4], strong magnetic field [5, 6], and high frequency [7], may exist in neutron stars. To describe their properties, the equation of state (EOS), namely, the relationship between energy density and pressure, of neutron-rich matter is needed. Great efforts have been devoted in both nuclear physics and astrophysics to understand the nature of neutron stars [4, 8–13]. In fact, to better constrain the underlying EOS of neutron star matter, many research facilities are currently operating, updating, or under construction around the world [14, 15], such as various advanced X-ray satellites and Earth-based large telescopes, the Neutron Star Interior Composition Explorer (NICER), various gravitational wave detectors, and advanced radioactive ion beam facilities. New observations and experiments at these facilities provide us with great opportunities to address some of the controversies regarding the EOS of neutron-rich matter especially at densities significantly higher than the saturation density ρ_0 of cold nuclear matter.

On the experimental and observational side, several useful constraints on the EOS at supra-saturation densities are known in addition to the empirical properties of nuclear matter around ρ_0. For example, the pressure of symmetric nuclear matter (SNM) has been constrained at densities between about 2 and 4.5 ρ_0 based on transport model analyses of the collective flow data in relativistic heavy-ion collisions [8]. In addition, kaon productions in heavy-ion reactions have provided additional constraints on the nuclear EOS at densities between 1.2 and 2.2 ρ_0 [16, 17]. However, the isospin-dependent part of the EOS of neutron-rich matter, i.e., the density dependence of nuclear symmetry energy $E_{\mathrm{sym}}(\rho)$, is less constrained so far. Moreover, the LIGO and Virgo Collaborations have recently extracted a bounding band on the EOS of neutron star matter based on their first direct detection of gravitational waves from the binary neutron star merger event GW170817. More quantitatively, the pressure at twice the nuclear saturation density was found to be $3.5^{+2.7}_{-1.7} \times 10^{34}$ dyn cm^{-2} at 90% confidence level [18]. We should note that all the reported EOS constraints are qualitatively consistent but suffer from large uncertainties.

On the theoretical side, essentially all existing nuclear many-body theories have been used to predict the EOS of neutron star matter using various interactions. For example, more than 500 EOSs from relativistic mean field (RMF) and Skyrme–Hartree–Fock calculations have been reported up to 2014 [19, 20]. However, even the EOSs for the simplest $npe\mu$ matter in neutron stars remain controversial, not to mention other particles or various phase transitions that may exist or occur in the core of neutron stars. This is mainly because of the large uncertainties associated with the symmetry energy E_{sym} [21, 22] especially at high densities. The symmetry energy has only been constrained around or below ρ_0. At higher density, neither the value nor the trend has been well determined yet. For most EOSs, the E_{sym} keeps increasing with density, but for some EOSs, the E_{sym} first increases and then remains constant or even decreases with density. It is thus important to take full advantage of the existing and forthcoming data to further constrain the EOS and the related $E_{\mathrm{sym}}(\rho)$.

Interestingly, great breakthroughs have been made in recent years in observing the properties of neutron stars, such as their masses [23, 24], radii [25], spin frequencies [7], tidal deformabilities [26], and moments of inertia [27]. While the existing constraints on the EOS and E_{sym} are mostly based on terrestrial nuclear laboratory experiments so far, fruitful efforts have also been devoted by many people to constrain the EOS and symmetry energy using astrophysical observations. Our recent contributions to this world-wide effort are based on an explicitly isospin-dependent parametric EOS [1–3]. Compared with using predictions based on various nuclear many-body theories, the parameterized EOS allows us to investigate some common issues and draw some useful conclusions independent of the particular many-body theories and/or interactions used. In addition to investigate the sensitivities of various astrophysical observables to the major features of the EOS of neutron star matter, we also make efforts to tackle the inverse-structure problem, i.e., using observational data to constrain the EOS parameters. In particular, we choose in the present work the mass, radius, and tidal deformability as the observational constraints to narrow down the EOS parameter space.

In our recent work, the following astrophysical observations were used to constrain the EOS parameters. The largest mass of observed neutron stars is about 2.0 $M_{\odot}$ [23, 24]. It provides a lower limit on the EOS and has ruled out many interactions. The radii of neutron stars remain controversial owing to many difficulties involved, such as determining the distance accurately and modeling the spectrum absorptions reliably with different atmosphere models in the X-ray observations. Nevertheless, many studies have been carried out to constrain the radius based on the thermal emissions from quiescent low-mass X-ray binaries and photospheric radius expansion bursts [28–33]. More recently, the first detection of a binary neutron star merger event GW170817 [18, 34–36, 36–41] has also led to new constraints on the radius for canonical neutron stars with a mass of 1.4 $M_{\odot}$. Interestingly, all the extracted radii are consistent and lie in the range of approximately 11–14 km. We adopt the range $10.62 < R_{1.4} < 12.83$ km from [25] in our studies. The tidal deformability Λ is uniquely determined by the EOS [42–45]. It can thus be used to constrain the EOS parameter space. Quantitatively, improved analyses of the GW170817 [26] estimated the dimensionless tidal deformability to be around $70 \le \Lambda_{1.4} \le 580$ for canonical neutron stars [18].

This paper is organized as follows: The details of constructing the EOS are presented in Sect. 2. Section 3 is devoted to narrowing down the EOS parameter space using the observations of mass, radius, and tidal deformability. The extracted constraints on the EOS and symmetry energy are discussed in Sect. 4, and a summary is given in Sect. 5.

2 Model framework for investigating the properties of neutron stars

As the available theories often predict different tendencies for the EOSs, the multi-parameter polytropic EOSs are widely used in modeling the core EOS of neutron stars

[46–50]. For example, a long time ago Topper [46] suggested a power-exponent EOS of the form

$$P = K\epsilon^{1+(1/n)} \tag{1}$$

where K and n are constants. A series of EOSs can be obtained by varying K and n; see, e.g., Refs. [51, 52]. Recently, Read et al. [48] considered a parametric EOS including several piecewise polytropes above ρ_0, namely,

$$P = K_i\epsilon^{\Gamma_i}, \quad d\frac{\epsilon}{\rho} = -P\frac{1}{\rho}, \quad \rho_{i-1} \le \rho \le \rho_i. \tag{2}$$

Each piece of the piecewise-polytropic EOS is specified by three parameters: the initial density, the coefficient K_i, and Γ_i. These parametric EOSs can be used to study the properties of neutron stars by solving the Tolman–Oppenheimer–Volkoff (TOV) equations. However, they are isospin independent. Since we are interested in understanding the inner compositions as well as the relationship between symmetry energy and the properties of neutron stars, we constructed an isospin-dependent parametric EOS in Ref. [1].

We start by using the so-called parabolic approximation for nucleon specific energy of asymmetric nuclear matter (ANM):

$$E_b(\rho,\delta) \approx E_0(\rho) + E_{\mathrm{sym}}(\rho)\delta^2, \tag{3}$$

where $E_0(\rho)$ is the nucleon specific energy in SNM and δ is the isospin asymmetry $\delta = (\rho_n - \rho_p)/\rho$. Next, we use the parameterizations

$$E_0(\rho) = E_0(\rho_0) + \frac{K_0}{2}\left(\frac{\rho-\rho_0}{3\rho_0}\right)^2 + \frac{J_0}{6}\left(\frac{\rho-\rho_0}{3\rho_0}\right)^3, \tag{4}$$

$$E_{\mathrm{sym}}(\rho) = E_{\mathrm{sym}}(\rho_0) + L\left(\frac{\rho-\rho_0}{3\rho_0}\right) + \frac{K_{\mathrm{sym}}}{2}\left(\frac{\rho-\rho_0}{3\rho_0}\right)^2 + \frac{J_{\mathrm{sym}}}{6}\left(\frac{\rho-\rho_0}{3\rho_0}\right)^3. \tag{5}$$

The above equations approach their Taylor expansions asymptotically when the density reaches ρ_0. In addition to the binding energy $E_0(\rho_0)$ of SNM and symmetry energy $E_{\mathrm{sym}}(\rho_0)$ at ρ_0, the other parameters involved have the asymptotic meanings of being the incompressibility K_0, skewness J_0 of SNM, as well as the slope L, curvature K_{sym}, and skewness J_{sym} of the symmetry energy.

The EOS of neutron star matter is the relationship between energy density and pressure. The energy density includes contributions from baryons and leptons:

$$\epsilon(\rho,\delta) = \epsilon_{\mathrm{b}}(\rho,\delta) + \epsilon_{\mathrm{l}}(\rho,\delta). \tag{6}$$

The energy density of baryons can be written as

$$\epsilon_{\mathrm{b}}(\rho,\delta) = \rho E_{\mathrm{b}}(\rho,\delta) + \rho M_{\mathrm{N}}, \tag{7}$$

where M_{N} is the average rest mass of nucleons. The isospin asymmetry δ in Eq. (3) is uniquely determined by $E_{\mathrm{sym}}(\rho)$ via

$$\mu_{\mathrm{n}} - \mu_{\mathrm{p}} = \mu_{\mathrm{e}} = \mu_\mu \approx 4\delta E_{\mathrm{sym}}(\rho), \tag{8}$$

where the chemical potential is defined as

$$\mu_i = \frac{\partial\epsilon(\rho,\delta)}{\partial\rho_i}. \tag{9}$$

Combining the above with the charge neutrality condition

$$\rho_{\mathrm{p}} = \rho_{\mathrm{e}} + \rho_\mu, \tag{10}$$

we can obtain the particle fractions at different densities of neutron stars core. Taking Eq. (3) into Eq. (7) and choosing $M_{\mathrm{N}} = 939$ MeV, the energy density of baryons can be obtained.

The energy density of leptons can be calculated based on the noninteracting Fermi gas model ($\hbar = c = 1$):

$$\epsilon_l(\rho,\delta) = \eta\phi(t) \tag{11}$$

with

$$\eta = \frac{m_{\mathrm{l}}^4}{8\pi^2}, \phi(t) = t\sqrt{1+t^2}(1+2t^2) - \ln\left(t+\sqrt{1+t^2}\right), \tag{12}$$

and

$$t = \frac{(3\pi^2\rho_{\mathrm{l}})^{1/3}}{m_{\mathrm{l}}}. \tag{13}$$

The pressure of the system can be calculated numerically by

$$P(\rho,\delta) = \rho^2\frac{\mathrm{d}\epsilon(\rho,\delta)/\rho}{\mathrm{d}\rho}. \tag{14}$$

Here, we have constructed a parametric EOS with parameters $E_0(\rho_0)$, $E_{\mathrm{sym}}(\rho_0)$, K_0, J_0, L, K_{sym}, and J_{sym}. We emphasize that if Eqs. (4) and (5) are considered as Taylor expansions, they indeed become progressively inaccurate for large densities and do not converge when $\rho > 1.5\rho_0$. However, since we regard them as parameterizations and all the coefficients are to be determined by the observations, we can still use Eqs. (4) and (5) to describe the high-density behavior of EOSs. Detailed demonstrations can be found in Ref. [1].

Among all the parameters, $E_0(\rho_0)$, K_0, $E_{\mathrm{sym}}(\rho_0)$, and L have been constrained by the terrestrial nuclear experiments. In particular, $E_0(\rho_0)$ is well accepted as ~ -16 MeV. Extensive studies over the last few decades have constrained the incompressibility of SNM as 240 ± 20 MeV [53, 54] or $K_0 = 230 \pm 40$ MeV [55]. The surveys of 53 analyses of different kinds of terrestrial and astrophysical data available up to 2016 have constrained the most probable values of $E_{\rm sym}(\rho_0)$ and L to be 31.7 ± 3.2 MeV and 58.7 ± 28.1 MeV, respectively. However, few constraints are available for the high-order parameters $K_{\rm sym}$, $J_{\rm sym}$, and J_0. Only several very rough constraints for J_0 are known based on different analyses in [28, 56], namely, $-1280 \leq J_0 \leq -10$ MeV, $-494 \leq J_0 \leq -10$ MeV, $-690 \leq J_0 \leq -208$ MeV, or $-790 \leq J_0 \leq -330$ MeV, respectively. They are generally consistent, but cover different ranges. Nevertheless, some calculations based on nuclear many-body theories have indicated that [1, 40, 57]: $-400 \leq K_{\rm sym} \leq 100$ MeV, $-200 \leq J_{\rm sym} \leq 800$ MeV, and $-800 \leq J_0 \leq 400$ MeV, respectively. It should be noted that some approximate relationships among the parameters of symmetry energy are suggested in [40, 58–64] based on the systematics of many predictions using various many-body theories and interactions. To focus on the effects of the high-density parameters on the properties of neutron stars and use the observational data to constrain the EOS parameter space, we fix the low-density parameters at their most probable values: $E_0(\rho_0) = -16$ MeV, $K_0 = 230$ MeV, $E_{\rm sym}(\rho_0) = 31.7$ MeV, and $L = 58.7$ MeV, while varying the high-density parameters within their uncertainty ranges of $-400 \leq K_{\rm sym} \leq 100$ MeV, $-200 \leq J_{\rm sym} \leq 800$ MeV, and $-800 \leq J_0 \leq 400$ MeV, respectively.

After obtaining the EOS from Eqs. (3), (11), and (14) for the core of neutron stars, we should connect it to the crust EOSs at the core–crust transition density and make sure that the baryon density, pressure, and energy density all keep increasing. More specifically, we use the NV EOS [65] for the inner crust and the BPS EOS [66] for the outer crust. The transition density can be calculated by the dynamical [66–69] or thermodynamical [70–72] methods. The transition density calculated from the thermodynamical method is slightly overestimated compared with the dynamical method, but this does not affect our conclusions. Thus, we choose the thermodynamical method in the present calculations. The incompressibility of neutron star matter can be expressed as

$$K_\mu = \rho^2 \frac{d^2 E_0}{d\rho^2} + 2\rho \frac{dE_0}{d\rho} + \delta^2 \left[\rho^2 \frac{d^2 E_{\rm sym}}{d\rho^2} + 2\rho \frac{dE_{\rm sym}}{d\rho} - 2E_{\rm sym}^{-1} \left(\rho \frac{dE_{\rm sym}}{d\rho} \right)^2 \right]. \tag{15}$$

A transition of K_μ from being positive to negative indicates the onset of dynamical instability in neutron star matter. As a result, cluster starts to form in the curst. Therefore, the core–crust transition density can be obtained by solving the condition $K_\mu = 0$. For more details, see Ref. [1].

With the EOS constructed consistently throughout the neutron star from its core to surface, the properties of neutron stars are obtained by solving the TOV equations [73, 74]

$$\frac{dP}{dr} = -\frac{G(m(r) + 4\pi r^3 P/c^2)(\epsilon + P/c^2)}{r(r - 2Gm(r)/c^2)}, \tag{16}$$

$$\frac{dm(r)}{dr} = 4\pi\epsilon r^2, \tag{17}$$

where G is the gravitation constant, c is the speed of light, and $m(r)$ is the gravitational mass enclosed within a radius r. The dimensionless tidal deformability Λ is related to the second Love number k_2, neutron star mass M, and radius R via

$$\Lambda = \frac{2}{3} k_2 \cdot \left(\frac{R}{M} \right)^5. \tag{18}$$

The tidal Love number k_2 depends on the stellar structure and can be calculated using a very complicated differential equation coupled to the TOV equation [42, 43]. More details about the formalism and code used in this work to calculate k_2 can be found in, e.g., [44, 45].

3 Observational constraints on the EOS parameter space

In this section, we study the combined constraints of neutron star mass, radius, and tidal deformability from astrophysical observations on the values of $K_{\rm sym}$, $J_{\rm sym}$, and J_0, namely, $M \geq 2.01$ M$_\odot$, $10.62 \leq R_{1.4} \leq 12.83$ km, and $70 \leq \Lambda_{1.4} \leq 580$, respectively. For this purpose, we first calculate the constraints of mass, radius, and tidal deformability in the $K_{\rm sym}$–$J_{\rm sym}$ plane with fixed J_0 and then the overall constraints are summarized in the three-dimensional parameter space of $K_{\rm sym}$–$J_{\rm sym}$–J_0. The crust and core EOSs are connected at the transition density. Moreover, the transition pressure is required to always remain positive, i.e., $P_{\rm t} \geq 0$ MeV, to maintain thermodynamical stability throughout the interior of neutron stars.

The constraints of mass, radius (left panel), and tidal deformability (right panel) in the $K_{\rm sym} - J_{\rm sym}$ plane with $J_0 = -100, 0, 100$, and 200 MeV, respectively, are shown in Fig. 1. The parameter space within the three lines are supported by the present observations. We can see from the left panel that $R_{1.4} = 12.83$ km can set an upper limit on the parameters and exclude larger $K_{\rm sym}$ and $J_{\rm sym}$ from the right side. While the lower limit $R_{1.4} = 10.62$ km shows more apparent effects from the left side for smaller $K_{\rm sym}$, effects of the mass constraint $M = 2.01$ M$_\odot$ become dominant for larger $K_{\rm sym}$. It is interesting to note that the slopes of the radius lines are larger than one, indicating that

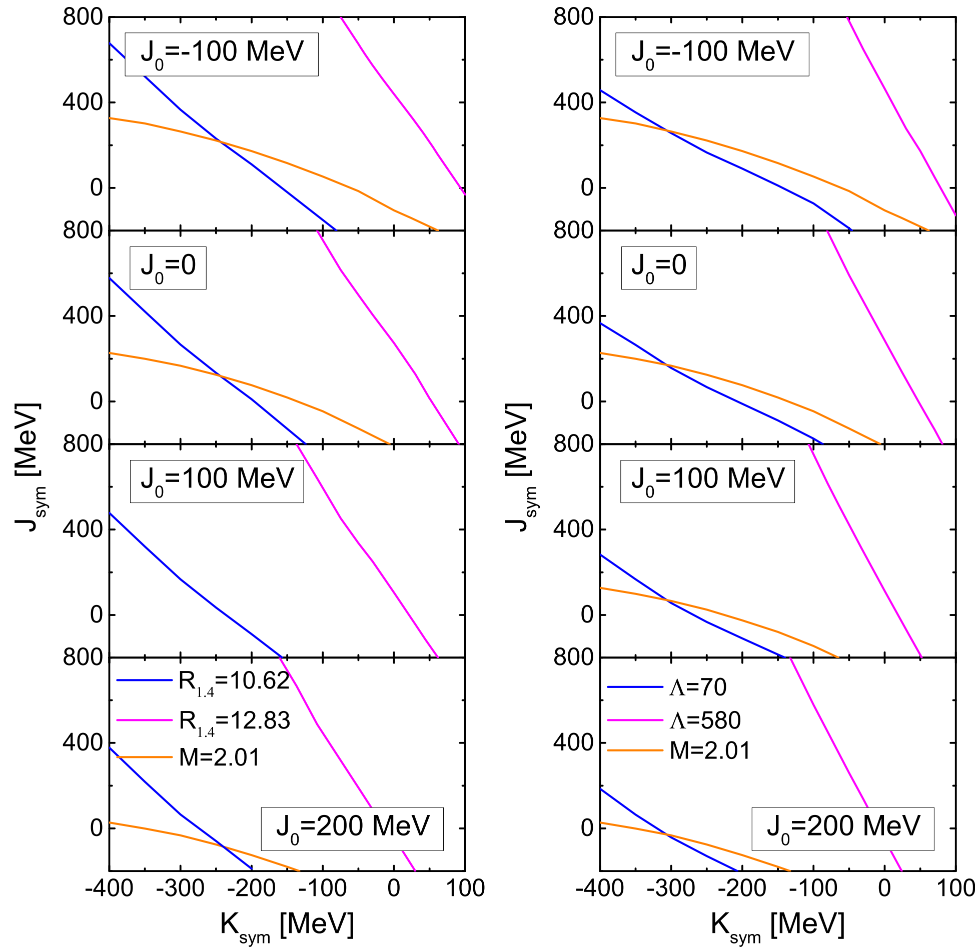

Fig. 1 The constraints of mass (in unit of $M_\odot$), radius (left panel, in unit of km), and tidal deformability (right panel) in the K_{sym}–J_{sym} plane with fixed $J_0 = -100, 0, 100$, and 200 MeV, respectively (Color online)

the radius depends more strongly on K_{sym} than J_{sym}. This is easy to understand because the central density of neutron stars with 1.4 $M_\odot$ is around several times ρ_0. Around such densities K_{sym} effectively determines the EOS while J_{sym} affects the EOS at higher densities. More quantitatively, by varying the J_0 from -100 to 200 MeV, the radius just shifts to the left slightly. On the other hand, the mass depends more strongly on the J_{sym} as we discuss in more detail later.

Similar tendencies for the tidal deformability can be seen in the right panel of Fig. 1. Comparing the left and right panels, it is seen that the radius shows stricter constraints on the parameters plane. Thus, the constraints of tidal deformability are consistent with but weaker than the radius constraints. Fortunately, future observations of more neutron star mergers are expected to help improve the constraints using the tidal deformabilities. In addition, based on the definition of Λ in Eq. (18), an underlying relation may exist between the $\Lambda_{1.4}$ and $R_{1.4}$. We note that in [34, 36, 37] it was suggested that $\Lambda_{1.4} \propto R_{1.4}^{\alpha}$ with α between about 5 and 7. However, our results shown in Fig. 1 demonstrate that the $\Lambda_{1.4}$–$R_{1.4}$ correlation does exist but is more linear. We refer the interested reader to [3] for a detailed discussion on this interesting issue.

To show the overall constraints on the K_{sym} and J_{sym} parameters for any value of J_0, the constant surfaces of $M = 2.01$ $M_\odot$ (green), $R_{1.4} = 10.62$ km (blue), and $R_{1.4} = 12.83$ km (magenta) are shown in the three-dimensional parameter space of K_{sym}–J_{sym}–J_0 in Fig. 2. As the constraints of radius are stronger than those of tidal deformability, we only show the constant surfaces of radius here. The arrows show the directions that satisfy the corresponding constraints. Take the surface of $R_{1.4} = 10.62$ km, for example, the constant surface means that all the points with different combinations of K_{sym}, J_{sym}, and J_0 on this surface lead to the same $R_{1.4} = 10.62$ km. The constant surface is numerically calculated as follows: In running the three loops through K_{sym}, J_{sym}, and J_0, we start from initializing $K_{sym} = -400$ MeV and $J_{sym} = -200$ MeV. Then, by varying J_0 from -800 to 400 MeV, we find the point generating a star with $M = 1.4$ $M_\odot$ and $R = 10.62$ km. Repeating the process by increasing in steps K_{sym} to 100 MeV and J_{sym} to 800 MeV, we find new combinations of the three parameters

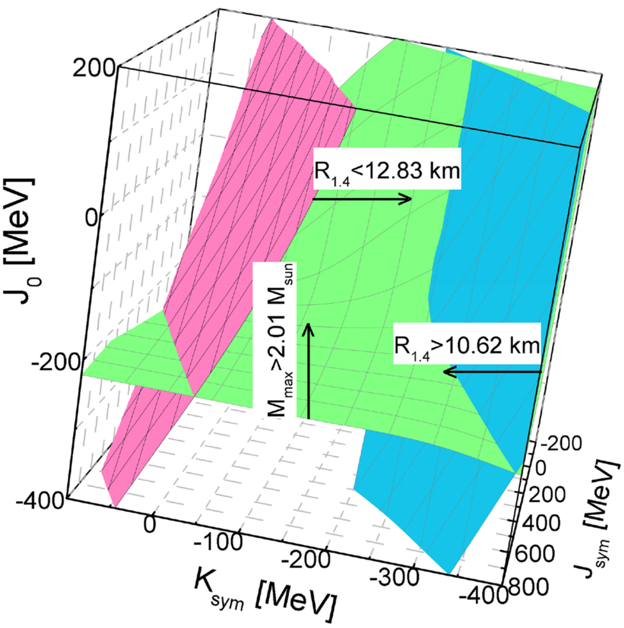

Fig. 2 Observational constraints of the maximum mass of neutron stars and the radius of canonical neutron stars on the EOS of dense neutron-rich matter in the K_{sym}, J_{sym}, and J_0 parameter space. The green, magenta, and orange surfaces represent $M = 2.01$ M$_\odot$, $R_{1.4} = 12.83$ km, and $R_{1.4} = 10.62$ km, respectively. Reproduced from [1] (Color online)

maintaining the configuration of $M = 1.4$ M$_\odot$ and $R = 10.62$ km. The constant surfaces of $M = 2.01$ M$_\odot$ and $R_{1.4} = 12.83$ km are calculated similarly.

Let us first focus on the constant surfaces of neutron star radius. It is well known that the radius of neutron stars with $M = 1.4$ M$_\odot$ depends strongly on the density dependence of nuclear symmetry energy, see, e.g., [75]. It is seen from Fig. 2 that the two surfaces are almost perpendicular to the K_{sym} axis. This is consistent with the results shown in Fig. 1 and supports the finding that $R_{1.4}$ is more sensitive/insensitive to K_{sym}/J_0 and thus more dependent on the symmetry energy $E_{sym}(\rho)$. When K_{sym} decreases, the EOS becomes softer if all other parameters are fixed. Thus, to support a neutron star of mass 1.4 M$_\odot$ with smaller K_{sym}, J_{sym} and J_0 have to be sufficiently large. This is the reason that the surfaces of constant radii incline toward the right side. To obtain larger radii, K_{sym} and J_{sym} should also be larger; thus, the surface of $R_{1.4} = 10.62$ km is on the right side of $R_{1.4} = 12.83$ km. It should be noted that L is fixed at its most probable value of 58.7 MeV in these calculations. The effects of changing the value of L within its own uncertainty range on constraining the EOS and symmetry energy are currently under investigation and will be reported elsewhere.

Next, let us examine the constant surface of $M = 2.01$ M$_\odot$. It is seen that the surface is rather flat with large J_{sym} regardless of the K_{sym} value. It then goes up toward the top right corner where K_{sym} and J_{sym} are both small. With the large K_{sym} and J_{sym} values, the symmetry energy is stiff. In this case, the isospin asymmetry δ of neutron star matter at β equilibrium is very small at high densities according to Eq. (8). Based on Eq. (3), δ^2 can significantly suppress the contributions from the symmetry energy, namely, K_{sym} and J_{sym}, to the total pressure. Thus, the constant mass surface is very flat and J_0 plays the dominant role when K_{sym} and J_{sym} are relatively large. When K_{sym} and J_{sym} become smaller, δ at high densities increases and can be 1 for super-soft symmetry energies. In this case, the symmetry energy plays a more important role in determining the total pressure. To support neutron stars with masses larger than 2.01 M$_\odot$, J_0 has to be large enough to sufficiently stiffen the EOS. Therefore, the constant mass surface bends upward to the top right corner.

The space surrounded by the three surfaces satisfies all the constraints from the mass, radius, and tidal deformability measurements considered in the present work. We can see that the EOS parameter space is apparently narrowed down, especially in the K_{sym} direction. However, more constraints from other observations or terrestrial experiments are needed to further restrict the EOS parameter space. In addition, the causality condition also provides natural constraints on the EOS parameter space as we discussed in detail in Ref. [2].

4 Constraining the EOS and symmetry energy of dense neutron-rich matter using astrophysical observations

The observational constraints discussed above can be used to set limits on the EOS and symmetry energy. Detailed discussions on our results can be found in Ref. [2]. While each observation may only limit the EOS in certain density region, or only provide an upper or lower limit, multiple observables together may lead to crosslines that help remove some degeneracies or provide complimentary information on the EOS. Taking the $R_{1.4} = 12.83$ km constraint, for example, as shown in Fig. 2, its intersection line with $M = 2.01$ M$_\odot$ surface sets a lower limit for the EOS parameters K_{sym}, J_{sym}, and J_0. In contrast, the causality surface provides an upper limit, see the right panel of Fig. 8 in Ref. [2]. Combining all the constraints of mass, radius, and causality (the tidal deformability is less constraining than the radius), all the points in the surrounded space or on the boundary surfaces can survive. The calculated EOSs and symmetry energy from these points can satisfy all the constraints, which means that the constraints on them can be extracted.

As an illustration of how the constraints can help limit the EOS, shown in Fig. 3 are 45 EOSs with parameters on the constrained $R_{1.4} = 12.83$ km surface. It is seen that for a certain density, both the upper and lower limits can be found for a given parameter set. By plotting a large number of EOSs constrained by the mass, radius, and causality all together, common upper and lower limits on the EOS satisfying all the constraints considered can be obtained for all densities relevant for neutron stars. In other words, we can generate a constrained band on the plot of energy density versus pressure. Similarly, the constrained band on symmetry energy can also be obtained, see Ref. [2] for details. To compare our constrained EOS with the constraint from LIGO + Virgo [18] (a constrained band on the plot of pressure as a function of baryon density), we transform our EOS into the pressure as a function of baryon density and plot the constraints we extracted with the shadowed range in Fig. 4. The upper and lower limits of the shadowed range are determined by the surfaces of causality and $M = 2.01$ $M_{\odot}$, respectively. The pressure extracted from the binary neutron star merger by the LIGO + Virgo Collaborations [18] is shown as the red boundary for a comparison. We can see that the two extracted boundaries of pressures in neutron stars are in good agreement. As we did not use the deformability in deriving the boundary of pressure, there is no self-correlation in comparison with the LIGO + Virgo results. Similarly, the upper and lower limits on nuclear symmetry energy at supra-saturation densities can also be extracted [2].

5 Summary

In summary, we have constructed an isospin-dependent parametric EOS for neutron star matter based on the parabolic approximation for nucleon specific energy in ANM. The low-order parameters ($E_0(\rho_0)$, K_0, $E_{\mathrm{sym}}(\rho_0)$, and L) characterizing the EOS and symmetry energy around the saturation density are fixed at their most probable values known mostly from terrestrial nuclear experiments, while the high-order parameters (K_{sym}, J_{sym}, and J_0) characterizing the high-density behaviors of nuclear EOS and symmetry energy are varied within their uncertain ranges based on predictions of nuclear many-body theories. We have found that the radius and tidal deformability of neutron stars with $M = 1.4$ $M_{\odot}$ depend appreciably on the K_{sym} and J_{sym} parameters while the L parameter plays a dominating role [3]. Moreover, the parametric EOS enables us to extract significant constraints on the EOS and nuclear symmetry energy from astrophysical observations. The EOS parameter space is significantly narrowed down by the astrophysical observations of the minimum–maximum mass $M = 2.01$ $M_{\odot}$, radius range of $10.62 \leq R_{1.4} \leq 12.83$ km, and the range of tidal deformability $70 \leq \Lambda_{1.4} \leq 580$ of neutron stars. In particular, the constraints on the pressure of neutron star matter extracted using the X-ray observations of neutron star radius, the minimum–maximum mass $M = 2.01$ $M_{\odot}$, and causality condition agree very well with those extracted from analyzing the tidal deformability data by the LIGO + Virgo Collaborations. As more observational data become available, the theoretical framework established in our recent work [1–3] is expected to be useful for establishing tighter constraints on the EOS and symmetry energy of dense neutron-rich matter.

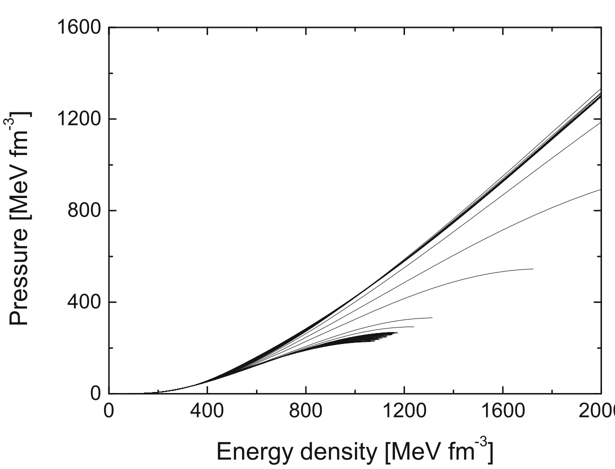

Fig. 3 45 examples of EOSs calculated from the parameter sets on the surface of $R_{1.4} = 12.83$ km

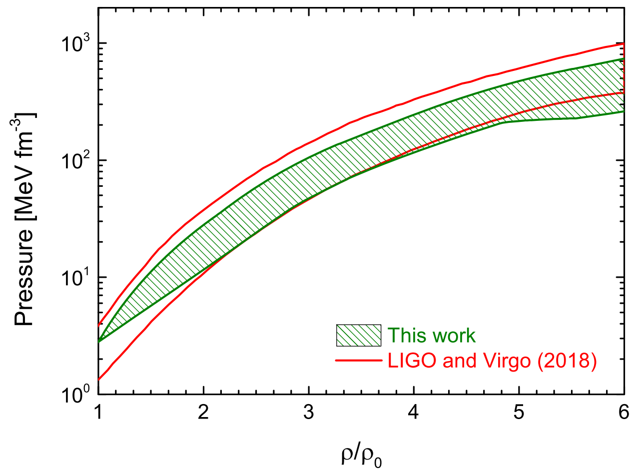

Fig. 4 Pressure (shaded region) as a function of baryon density in neutron star matter at β equilibrium extracted using the recent X-ray observations of neutron star radii, known minimum–maximum mass of neutron stars and the causality condition in comparison with the LIGO + Virgo result at 90% confidence level (red boundary) using their measurement of the tidal deformabilities [18]. Reproduced from [2] (Color online)

Acknowledgements We would like to thank Prof. Lie-Wen Chen, Plamen G. Krastev, Bin Qi, De-Hua Wen, and Jun Xu for their helpful discussions.

References

1. N.B. Zhang, B.A. Li, J. Xu, Combined constraints on the equation of state of dense neutron-rich natter from terrestrial nuclear experiments and observations of neutron stars. Astrophys. J. **859**, 90 (2018). https://doi.org/10.3847/1538-4357/aac027
2. N.B. Zhang, B.A. Li, Extracting nuclear symmetry energies at high densities from observations of neutron stars and gravitational waves. arXiv:1807.07698v1
3. N.B. Zhang, B.A. Li, Delineating effects of nuclear symmetry energy on the radii and tidal deformabilities of neutron stars. J. Phys. G in press arXiv:1808.07955v1
4. J.M. Lattimer, M. Prakash, The equation of state of hot, dense matter and neutron stars. Phys. Rep. **621**, 127–164 (2016). https://doi.org/10.1016/j.physrep.2015.12.005
5. R.C. Duncan, C. Thompson, Formation of very strongly magnetized neutron stars-implications for gamma-ray bursts. Astrophys. J. **392**, L9-13 (1992). http://adsabs.harvard.edu/abs/1992ApJ...392L...9D
6. C. Thompson, R.C. Duncan, Neutron star dynamos and the origins of pulsar magnetism. Astrophys. J. **408**, 194–217 (1993). http://adsabs.harvard.edu/abs/1993ApJ...408..194T
7. J.W.T. Hessels, S.M. Ransom, I.H. Stairs et al., A radio pulsar spinning at 716 Hz. Science **311**, 1901–1904 (2006). https://doi.org/10.1007/s41365-017-0329-1
8. P. Danielewicz, R. Lacey, W.G. Lynch, Determination of the equation of state of dense matter. Science **298**, 1592–1596 (2002). https://doi.org/10.1126/science.1078070
9. A.L. Watts, N. Andersson, D. Chakrabarty et al., Colloquium: measuring the neutron star equation of state using x-ray timing. Rev. Mod. Phys. **88**, 021001 (2016). https://doi.org/10.1103/RevModPhys.88.021001
10. M. Oertel, M. Hempel, T. Klähn, S. Typel, Equations of state for supernovae and compact stars. Rev. Mod. Phys. **89**, 015007 (2017). https://doi.org/10.1103/RevModPhys.89.015007
11. F. Özel, P. Freire, Masses, radii, and the equation of state of neutron stars. Annu. Rev. Astron. Astrophys. **54**, 401 (2016). https://doi.org/10.1146/annurev-astro-081915-023322
12. B.A. Li, Nuclear symmetry energy extracted from laboratory experiments. Nucl. Phys. News **27**, 7 (2017). https://doi.org/10.1080/10619127.2017.1388681
13. D. Blaschke, N. Chamel, Phases of dense matter in compact stars. arXiv:1803.01836
14. National Research Council, *New Worlds, New Horizons in Astronomy and Astrophysics* (The National Academies Press, Washington, DC, 2010). https://doi.org/10.17226/12951
15. National Research Council, *Nuclear Physics: Exploring the Heart of Matter* (The National Academies Press, Washington, DC, 2013). https://doi.org/10.17226/13438
16. C. Fuchs, Kaon production in heavy ion reactions at intermediate energies. Prog. Part. Nucl. Phys. **56**, 1–103 (2006). https://doi.org/10.1016/j.ppnp.2005.07.004
17. W.G. Lynch, M.B. Tsang, Y. Zhang et al., Probing the symmetry energy with heavy ions. Prog. Part. Nucl. Phys. **62**, 427–432 (2009). https://doi.org/10.1016/j.ppnp.2009.01.001
18. The LIGO Scientific Collaboration, Virgo Collaboration, GW170817: measurements of neutron star radii and equation of state. Phys. Rev. Lett. **121**, 161101 (2018). https://doi.org/10.1103/PhysRevLett.121.161101
19. M. Dutra, O. Louren, J.S.S. Martins et al., Skyrme interaction and nuclear matter constraints. Phys. Rev. C **85**, 035201 (2012). https://doi.org/10.1103/PhysRevC.85.035201
20. M. Dutra, O. Louren, S.S. Avancini et al., Relativistic mean-field hadronic models under nuclear matter constraints. Phys. Rev. C **90**, 055203 (2014). https://doi.org/10.1103/PhysRevC.90.055203
21. B.A. Li, À. Ramos, G. Verde, I. Vidaña, Topical issue on nuclear symmetry energy. Eur. Phys. J. A **50**, 9 (2014). https://doi.org/10.1140/epja/i2014-14009-x
22. L.W. Chen, Symmetry energy in nucleon and quark matter. Nucl. Phys. Rev. **34**, 20 (2017). https://doi.org/10.11804/NuclPhysRev.34.01.020
23. P.B. Demorest, T. Pennucci, S.M. Ransom et al., A two-solar-mass neutron star measured using Shapiro delay. Nature **467**, 1081–1083 (2010). https://doi.org/10.1038/nature09466
24. J. Antoniadis, P.C.C. Freire, N. Wex et al., A massive pulsar in a compact relativistic binary. Science **340**, 448 (2013). https://doi.org/10.1126/science.1233232
25. J.M. Lattimer, A.W. Steiner, Constraints on the symmetry energy using the mass–radius relation of neutron stars. Eur. Phys. J. A **50**, 40 (2014). https://doi.org/10.1140/epja/i2014-14040-y
26. B.P. Abbott, R. Abbott, T.D. Abbott et al., (LIGO Scientific Collaboration and Virgo Collaboration) GW170817: observation of gravitational waves from a binary neutron star inspiral. Phys. Rev. Lett. **119**, 161101 (2017). https://doi.org/10.1103/PhysRevLett.119.161101
27. B. Link, R.I. Epstein, J.M. Lattimer, Pulsar constraints on neutron star structure and equation of state. Phys. Rev. Lett. **83**, 3362 (1999). https://doi.org/10.1103/PhysRevLett.83.3362
28. A.W. Steiner, J.M. Lattimer, E.F. Brown, The equation of state from observed massed and radii of neutron stars. Astrophys. J. **722**, 33 (2010). https://doi.org/10.1088/0004-637X/722/1/33
29. F. Özel, D. Psaltis, T. Güver et al., The dense matter equation of state from neutron star radius and mass measurements. Astrophys. J. **820**, 28 (2016). https://doi.org/10.3847/0004-637X/820/1/28
30. S. Bogdanov, C.O. Heinke, F. Özel et al., Neutron star mass–radius constraints of the quiescent low-mass X-ray binaries X7 and X5 in the globular cluster 47 Tuc. Astrophys. J. **831**, 184 (2016). https://doi.org/10.3847/0004-637X/831/2/184
31. C.A. Raithel, F. Özel, D. Psaltis, From neutron star observations to the equation of state I. An optimal parametrization. Astrophys. J. **831**, 44 (2016). https://doi.org/10.3847/0004-637X/831/1/44
32. C.A. Raithel, F. Özel, D. Psaltis, From neutron star observations to the equation of state. II. Bayesian inference of equation of state pressures. Astrophys. J. **844**, 156 (2017). https://doi.org/10.3847/1538-4357/aa7a5a
33. A.W. Steiner, C.O. Heinke, S. Bogdanov et al., Constraining the mass and radius of neutron stars in globular clusters. Mont. Not. R. Astron. Soc. **476**, 421 (2018). https://doi.org/10.1093/mnras/sty215
34. F.J. Fattoyev, J. Piekarewicz, C.J. Horowitz, Neutron skins and neutron stars in the multimessenger era. Phys. Rev. Lett. **120**, 172702 (2018). https://doi.org/10.1103/PhysRevLett.120.172702
35. E.R. Most, L.R. Weih, L. Rezzolla et al., New constraints on radii and tidal deformabilities of neutron stars from GW170817. Phys. Rev. Lett. **120**, 261103 (2018). https://doi.org/10.1103/PhysRevLett.120.261103
36. T. Malik, N. Alam, M. Fortin, et al., GW170817: constraining the nuclear matter equation of state from the neutron star tidal deformability. arXiv:1805.11963
37. E. Annala, T. Gorda, A. Kurkela et al., Gravitational-wave constraints on the neutron-star-matter equation of State. Phys. Rev. Lett. **120**, 172703 (2018). https://doi.org/10.1103/PhysRevLett.120.172703
38. P.G. Krastev, B.A. Li, Imprints of the nuclear symmetry energy on the tidal deformability of neutron stars. arXiv:1801.04620
39. C. Raithel, F. Özel, D. Psaltis, GW170817: joint constraint on the neutron star equation of state from multimessenger observations. Astrophys. J. Lett. **857**, L23 (2018). https://doi.org/10.3847/2041-8213/aaa402

40. I. Tews, J. Margueron, S. Reddy, How well does GW170817 constrain the equation of state of dense matter? arXiv:1804.02783
41. Y. Lim, J.W. Holt, Neutron star tidal deformabilities constrained by nuclear theory and experiment. Phys. Rev. Lett. **121**, 062701 (2018). https://doi.org/10.1103/PhysRevLett.121.062701
42. T. Hinderer, Tidal love numbers of neutron stars. Astrophys. J. **677**, 1216 (2008). https://doi.org/10.1088/0004-637X/697/1/964
43. T. Hinderer, B.D. Lackey, R.N. Lang et al., Tidal deformability of neutron stars with realistic equations of state and their gravitational wave signatures in binary inspiral. Phys. Rev. D **81**, 123016 (2010). https://doi.org/10.1103/PhysRevD.81.123016
44. F.J. Fattoyev, J. Carvajal, W.G. Newton et al., Constraining the high-density behavior of nuclear symmetry energy with the tidal deformability of neutron stars. Phys. Rev. C **87**, 015806 (2013). https://doi.org/10.1103/PhysRevC.87.015806
45. F.J. Fattoyev, W.G. Newton, B.A. Li, Probing the high-density behavior of symmetry energy with gravitational waves. Eur. Phys. J. A **50**, 45 (2014). https://doi.org/10.1140/epja/i2014-14045-6
46. R.F. Topper, General relativistic polytropic fluid spheres. Astrophys. J. **140**, 434 (1964). https://doi.org/10.1086/147939
47. E.M. Butterworth, On the structure and stability of rapidly rotating fluid bodies in general relativity. II—the structure of uniformly rotating pseudopolytropes. Astrophys. J. **204**, 561 (1976). https://doi.org/10.1086/154204
48. J.S. Read, B.D. Lackey, B.J. Owen et al., Constraints on a phenomenologically parametrized neutron-star equation of state. Phys. Rev. D **79**, 124032 (2009). https://doi.org/10.1103/PhysRevD.79.124032
49. J. Margueron, R.H. Casali, F. Gulminelli, Equation of state for dense nucleonic matter from metamodeling. I. Foundational aspects. Phys. Rev. C **97**, 025805 (2017). https://doi.org/10.1103/PhysRevC.97.025805
50. J. Margueron, R.H. Casali, F. Gulminelli, Equation of state for dense nucleonic matter from metamodeling. II. Predictions for neutron star properties. Phys. Rev. C **97**, 025806 (2017). https://doi.org/10.1103/PhysRevC.97.025806
51. K. Hidemi, E. Yoshiharu, H. Izumi, Rapidly rotating general relativistic stars. I—numerical method and its application to uniformly rotating polytropes. Mont. Not. R. Astron. Soc. **237**, 355–379 (1989). https://doi.org/10.1093/mnras/237.2.355
52. G.B. Cook, S.L. Shapiro, S.A. Teukolsky, Rapidly rotating polytropes in general relativity. Astrophys. J. **422**, 227 (1994). https://doi.org/10.1086/173721
53. S. Shlomo, V.M. Kolomietz, G. Coló, Deducing the nuclear-matter incompressibility coefficient from data on isoscalar compression modes. Eur. Phys. J. A **30**, 23 (2006). https://doi.org/10.1140/epja/i2006-10100-3
54. J. Piekarewicz, Do we understand the incompressibility of neutronrich matter? J. Phys. G **37**, 064038 (2010). https://doi.org/10.1088/0954-3899/37/6/064038
55. E. Khan, J. Margueron, I. Vidaña, Constraining the nuclear equation of state at subsaturation densities. Phys. Rev. Lett. **109**, 092501 (2012). https://doi.org/10.1103/PhysRevLett.109.092501
56. B.J. Cai, L.W. Chen, Constraints on the skewness coefficient of symmetric nuclear matter within the nonlinear relativistic mean field model. Nucl. Sci. Technol. **28**, 185 (2017). https://doi.org/10.1007/s41365-017-0329-1
57. N.B. Zhang, B.J. Cai, B.A. Li et al., How tightly is the nuclear symmetry energy constrained by a unitary Fermi gas? Nucl. Sci. Technol. **28**, 181 (2017). https://doi.org/10.1007/s41365-017-0336-2
58. M. Farine, J.M. Pearson, B. Rouben, Higher-order volume-symmetry terms of the mass formula. Nucl. Phys. **304**, A317–326 (1978). https://doi.org/10.1016/0375-9474(78)90241-5
59. L.W. Chen, B.J. Cai, C.M. Ko et al., Higher-order effects on the incompressibility of isospin asymmetric nuclear matter. Phys. Rev. C **80**, 014322 (2009). https://doi.org/10.1103/PhysRevC.80.014322
60. P. Danielewicz, J. Lee, Symmetry energy I: semi-infinite matter. Nucl. Phys. **818**, A36–96 (2009). https://doi.org/10.1016/j.nuclphysa.2008.11.007
61. I. Vidaña, C. Providência, A. Polls et al., Density dependence of the nuclear symmetry energy: a microscopic perspective. Phys. Rev. C **80**, 045806 (2009). https://doi.org/10.1103/PhysRevC.80.045806
62. C. Ducoin, J. Margueron, C. Providência et al., Core-crust transition in neutron stars: predictivity of density developments. Phys. Rev. C **83**, 045810 (2011). https://doi.org/10.1103/PhysRevC.83.045810
63. C. Providência, S.S. Avancini, R. Cavagnoli et al., Imprint of the symmetry energy on the inner crust and strangeness content of neutron stars. Euro. Phys. J. A **50**, 1–18 (2014). https://doi.org/10.1140/epja/i2014-14044-7
64. C. Mondal, B.K. Agrawal, J.N. De et al., Interdependence of different symmetry energy elements. Phys. Rev. C **96**, 021302(R) (2017). https://doi.org/10.1103/PhysRevC.96.021302
65. J.W. Negele, D. Vautherin, Neutron star matter at sub-nuclear densities. Nucl. Phys. **207**, A298–320 (1973). https://doi.org/10.1016/0375-9474(73)90349-7
66. G. Baym, C.J. Pethick, P. Sutherland, The ground state of matter at high densities: equation of state and stellar models. Astrophys. J. **170**, 299 (1971). https://doi.org/10.1086/151216
67. G. Baym, H.A. Bethe, C.J. Pethick, Neutron star matter. Nucl. Phys. **175**, A225–271 (1971). https://doi.org/10.1016/0375-9474(71)90281-8
68. C.J. Pethick, D.G. Ravenhall, C.P. Lorenz, The inner boundary of a neutron-star crust. Nucl. Phys. **584**, A675–703 (1995). https://doi.org/10.1016/0375-9474(94)00506-I
69. C. Ducoin, Ph Chomaz, F. Gulminelli, Isospin-dependent clusterization of neutron-star matter. Nucl. Phys. **789**, A403–425 (2007). https://doi.org/10.1016/j.nuclphysa.2007.03.006
70. S. Kubis, Diffusive instability of a kaon condensate in neutron star matter. Phys. Rev. C **70**, 065804 (2004). https://doi.org/10.1103/PhysRevC.70.065804
71. S. Kubis, Nuclear symmetry energy and stability of matter in neutron stars. Phys. Rev. C **76**, 035801 (2007). https://doi.org/10.1103/PhysRevC.76.025801
72. J.M. Lattimer, M. Prakash, Neutron star observations: prognosis for equation of state constraints. Phys. Rep. **442**, 109 (2007). https://doi.org/10.1016/j.physrep.2007.02.003
73. R.C. Tolman, Effect of inhomogeneity on cosmological models. Proc. Natl. Acad. Sci. U. S. A. **20**, 169–176 (1934). https://doi.org/10.1073/pnas.20.3.169
74. J. Oppenheimer, G. Volkoff, On massive neutron cores. Phys. Rev. **55**, 374–381 (1939). https://doi.org/10.1103/PhysRev.55.374
75. B.A. Li, A.W. Steiner, Constraining the radii of neutron stars with terrestrial nuclear laboratory data. Phys. Lett. **642**, B436–440 (2006). https://doi.org/10.1016/j.physletb.2006.09.065